ACS OMEGA

Article

Cite This: ACS Omega 2018, 3, 1102−1109

Solar Paint from TiO_2 Particles Supported Quantum Dots for Photoanodes in Quantum Dot−Sensitized Solar Cells

Gencai Shen,[†] Zhonglin Du,[†] Zhenxiao Pan,*[,‡] Jun Du,[†] and Xinhua Zhong*[,†,‡]

[†]School of Chemistry and Molecular Engineering, East China University of Science and Technology, 130 Meilong Road, Shanghai 200237, China

[‡]College of Materials and Energy, South China Agricultural University, 483 Wushan Road, Guangzhou 510642, China

Supporting Information

ABSTRACT: The preparation of quantum dot (QD)−sensitized photoanodes, especially the deposition of QDs on TiO_2 matrix, is usually a time-extensive and performance-determinant step in the construction of QD-sensitized solar cells (QDSCs). Herein, a transformative approach for immobilizing QD on the TiO_2 matrix was developed by simply mixing the as-prepared oil-soluble QDs with TiO_2 P25 particles suspension for a period as short as half a minute. The solar paint was prepared by adding the TiO_2/QD composite in a binder solution under ultrasonication. The QD-sensitized photoanodes were then obtained by simply brushing the solar paint on a fluorine-doped tin oxide substrate followed by a low-temperature annealing at ambient atmosphere. Sandwich-structured complete QDSCs were assembled with the use of Cu_2S/brass as counter electrode and polysulfide redox couple as an electrolyte. The photovoltaic performance of the resulting Zn−Cu−In−Se (ZCISe) QDSCs was evaluated after primary optimization of the QD/TiO_2 ratio as well as the thicknesses of photoanode films. In this proof of concept with a simple solar paint approach for photoanode films, an average power conversion efficiency of 4.13% (J_{sc} = 11.11 mA/cm^2, V_{oc} = 0.590 V, fill factor = 0.631) was obtained under standard irradiation condition. This facile solar paint approach offers a simple and convenient approach for QD-sensitized photoanodes in the construction of QDSCs.

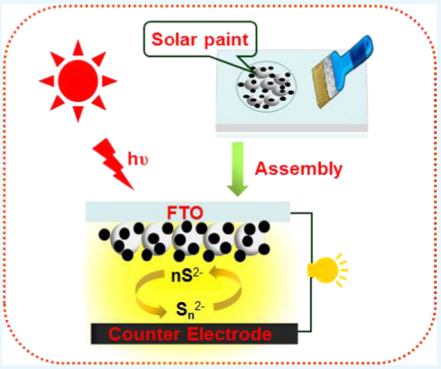

INTRODUCTION

The development of high-efficiency and low-cost photovoltaic cells is an effective way to solve the increasing concerns on global warming and the exhaustion of fossil fuels.[1,2] Quantum dot−sensitized solar cells (QDSCs) are considered as one of the promising third-generation solar cells due to the excellent optoelectronic properties of QD light absorbers, such as high absorption coefficient, tunable light-harvesting range, high stability, and low-cost availability.[2−6] Furthermore, due to the multiexciton generation possibility, the theoretical maximum power conversion efficiency (PCE) of QDSCs can go beyond the Shockley−Queisser limit and reach 44%.[7,8] The structure of QDSCs is similar to that of dye-sensitized solar cells with a light-harvesting material-sensitized photoanode, electrolyte, and a counter electrode. In the photoanode, light-harvesting material QDs are immobilized on nanocrystallite metal oxide (mainly TiO_2) mesoporous films. The mesoporous film electrode plays a crucial role in determining the performance of a cell device, such as providing enormous surface areas for supporting enough amounts of QD light absorbers, collecting and transmitting photogenerated electrons, and allowing redox couple electrolyte penetrating into the interior of the film to regenerate QD sensitizers.[9] Usually, a series of time-consuming procedures are required to get access to a well-performing photoanode. First, crystallite TiO_2 mesoporous film electrodes are prepared by coating TiO_2 paste on an optically transparent electrode (herein, fluorine-doped tin oxide (FTO) conducting glass) substrate and following a high-temperature sintering process.[10,11] Then, QD sensitizers are immobilized on the film electrode. This QD deposition step is considered as a crucial and challenging step in determining the photovoltaic performance of the resultant cell device.[12−14]

Currently, two major routes, i.e., in situ growth, and postsynthesis assembly with use of preprepared QDs, have been developed for the immobilization of QDs on a mesoporous film electrode.[13−27] For the first route, QDs are formed in situ on a mesoporous TiO_2 film electrode starting from a solution containing the corresponding cationic and anionic precursors for QDs.[15−20] For the second one, the preprepared QDs are tethered on the film electrode via direct adsorption, molecular linker-, or electrophoresis-assisted assembly process.[21−27] Benefiting from the feasible penetration of ionic precursors into the nanoscaled channels of the mesoporous film electrode, in situ growth route can result in an effective and high coverage of QD on the electrode surface.[28] However, the drawback of this route is the high density of trap state defects and heterogeneous size distribution of the formed QDs. These disadvantages limit the photovoltaic

Received: November 10, 2017
Accepted: January 16, 2018
Published: January 26, 2018

DOI: 10.1021/acsomega.7b01761
ACS Omega 2018, 3, 1102−1109

performance of the resulting cell devices. In contrast, the postsynthesis assembly route is favored by the high quality of the preprepared QDs, but is shadowed by the low uploading amount of QDs due to the relatively large size of QD particles.[29−32] The deposition of QD sensitizers on the mesoporous film electrodes has thus being a bottleneck in the development of high-efficiency QDSCs.

To construct versatile and low-cost QDSCs, it is necessary to simplify the currently delicate and time-intensive preparation procedure for photoanodes, especially the QD sensitization procedure. Unambiguously, the invention that QD-sensitized photoanodes can be attained by simply brushing a solar paint on a conductive substrate is a transformative step in manufacturing QDSCs. This pioneering concept was tried by Hodes and co-workers.[33] They developed a solar paint using CdSe, CdTe powder with a fluxing material such as $CdCl_2$, but the corresponding photovoltaic performance was not obtained. Recently, Kamat and co-workers reported solar paints for photoanode by simply mixing the commercially available TiO_2 P25 powder with bulk CdS powder in water and *t*-butanol mixture solvent or depositing CdS (or CdSe) nanoparticles on the suspended P25 particles by adsorption of Cd^{2+} and S^{2-} (or Se^{2-}) ions alternatively. The obtained highest PCE was 1.08% in their work.[34] During the preparation of this article, Bang and co-workers increased the highest PCE to 1.35% through this solar paint route with use of PbS QDs as the light-harvesting material.[35] However, all of these reported solar paint approaches to fabricate the photoanode applied the successive ion layer absorption and reaction method to deposit QDs on the TiO_2 substrate. As discussed above, this in situ growth method usually resulted in the high density of trap state defects and heterogeneous size distribution of the formed QDs, seriously deteriorating photovoltaic performance of the cell devices. Thus, preparing solar paint with use of presynthesized high-quality QDs owns a great potential to obtain high-efficiency QDSC based on solar paint.

Herein, we target at simplifying the preparation procedure of QD-sensitized photoanode by simply brushing a solar paint on the FTO substrate, followed by a low temperature annealing treatment at ambient atmosphere. The solar paint was made from TiO_2/QD composites, which were obtained by direct adsorption of presynthesized oil-soluble QDs on the TiO_2 P25 suspension in a period as short as half a minute. Less-toxic and environmental-benign Zn−Cu−In−Se (ZCISe) QDs were selected as the model QD light absorber. An average PCE of 4.13% was achieved in the resulting QDSCs with use of Cu_2S/brass counter electrode.

RESULTS AND DISCUSSION

Solar Paint and Photoanode Preparation. In QDSCs, the QD-sensitized photoanodes are normally prepared by tethering QD on TiO_2 nanocrystallite mesoporous films.[15−27] On one hand, the adopted mesoporous structured film can enormously enhance the surface face of the matrix for supporting much more QDs, and therefore improving the light-harvesting capability; on the other hand, the nanoscale channel throughout the film renders the QD deposition process difficult and time-consuming. To overcome the disadvantage of the conventional route in the preparation of photoanodes, herein QD sensitizers are immobilized on the suspending TiO_2 P25 particles to get the TiO_2 particles supported QD composite powder (noted as TiO_2/QD hereafter). Then, the obtained TiO_2/QD powder is mixed with a binder solution to get the so-called solar paint. From this solar paint, QD-sensitized photoanodes could be feasibly obtained via a screen printing process. Scheme 1 illustrates the preparation of QD-sensitized photoanodes with use of solar paint starting from the TiO_2/QD composite powder.

Scheme 1. Schematic Procedure for the Preparation of QD-Sensitized Photoanodes

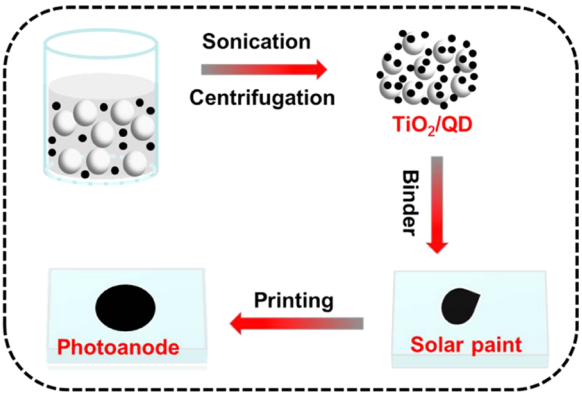

In the experiment, oleylamine (OAm) capped oil-soluble ZCISe QD light-harvesting materials with particle size of 4.1 nm and absorption onset of 980 nm are first synthesized according to literature method.[32,38] The corresponding optical spectra are available in Figure S1. Then, a fixed amount of P25 (0.5 g) suspension in CH_2Cl_2 is mixed with ZCISe QD dispersion in CH_2Cl_2 to get the TiO_2/QD composite. To get an optimal loading amount, the amount of QD used is varied. Without the limitation of nanoscaled narrow channels, as encountered in previously commonly used mesoporous film,[15−27] in our case, both QD and P25 particles are suspended in the solution; therefore, QDs could get access and tether on P25 particles from any direction. As a result, the deposition of QD on P25 could be completed in a period as less as 30 s. Meanwhile, a high loading amount of QD on the P25 particles can also be obtained as discussed below. It is highlighted that in this work the initial OAm-capped oil-soluble QDs are used directly in this sensitization process. Due to the chemical inertness of the long hydrocarbon chain in OAm ligand around QDs, the deposition of oil-soluble QD on the conventional TiO_2 film electrode is usually an extensively time-consuming process with the deposition time up to several even to tens of hours, as well as a low uploading amount.[39−44]

To avoid the degradation of ZCISe QDs at the following high-temperature annealing process, a recipe for binder solution borrowed from the paste suitable for conducting polymer substrate is adopted in the preparation of solar paint in our case.[36] In the experiment, solar paint is obtained by adding TiO_2/QD powder to a poly(vinylidene difluoride) (PVDF) binder solution under ultrasonication. The resulting thick, brown solar paint could then be screen printed directly on FTO to obtain QD-sensitized photoanodes after a low-temperature (120 °C) annealing process. TiO_2/QD powder is obtained by direct adsorption of the initial oil-soluble QD on the P25 particles suspension. The solar paint is then prepared by mixing the obtained TiO_2/QD powder with a PVDF binder solution. Finally, the photoanodes are obtained by screen printing the solar paint on the FTO substrate followed with a 120 °C annealing procedure at ambient atmosphere for 1 h. It is noted that this low annealing temperature cannot eliminate the PVDF

DOI: 10.1021/acsomega.7b01761
ACS Omega 2018, 3, 1102−1109

completely, rendering the PVDF to remain in the photoanode film. The insulating feature of the PVDF in the intervals among neighboring TiO_2 particles hinders the photogenerated transportation among the TiO_2 particles and decrease the photovoltaic performance accordingly. Thus, the amount of PVDF in the solar paint is optimized, and it is found that the addition of 20 mg PVDF gives the best photovoltaic performance. The corresponding photovoltaic parameters of QDSCs prepared with different amounts of PVDF in the solar paint are shown in Table S3. On the basis of these obtained photoanodes, the sandwich-structured complete cells are assembled with the use of Cu_2S/brass counter electrode, and the corresponding photovoltaic performances are evaluated.

Figure 1 shows the absorption spectra of ZCISe QD-sensitized TiO_2 film electrodes derived from different amounts

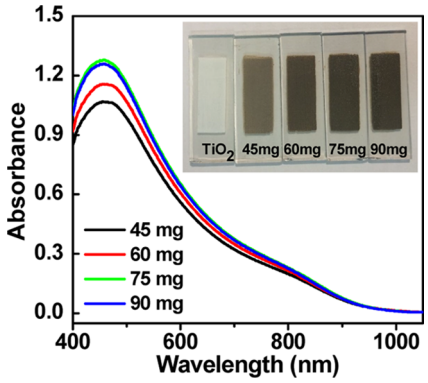

Figure 1. UV−vis absorption spectra of TiO_2 film corresponding to different contents of ZCISe QDs in the TiO_2 suspension. Inset: photographs of corresponding film electrodes.

of ZCISe QDs used in the preparation of TiO_2/QD composite. It is found that with the increase in the QD amount in the TiO_2 suspension, the absorbance in the resulting film electrode with identical thickness is improved accordingly to reach a saturation value at the QD amount of 75.0 mg. This indicates that the increase in QD loading on the TiO_2 particles is translated into the enhancement of loading amount on the final film electrode. For convenience, the used QD amount in the TiO_2 suspension is used to distinguish the loading amount in film electrodes hereafter. The increase in absorbance in the photoanode film indicates the enhancement of QD loading amount on the TiO_2 particles, and also the improvement of the light-harvesting capacity of the film electrode. The enhancement of QD loading amount of P25 can also be reflected by the deepening of the photograph color of the film electrode, as shown in the inset of Figure 1. Similar to the case of the absorption spectra from the QD dispersion in CH_2Cl_2 (Figure S1), the light absorption range for the resulting photoanodes covers the whole visible spectrum and expands to the near-infrared window with the longest wavelength extending to near 1000 nm. This excellent light-harvesting capacity paves the way for achieving an outstanding photovoltaic performance of the resulting cell devices as discussed below.

Figure 2a shows the transition electron microscopy (TEM) images of ZCISe QDs-sensitized TiO_2 film electrodes. From the TEM images, it can be seen that the surface of P25 particles (about 20−50 nm) is covered densely by smaller spherical particles (ZCISe QD, about 4 nm). This gives a visual evidence for the uniform distribution of QDs onto the P25 particles. Figure 2b shows the cross-sectional field emission scanning electron microscopy (SEM) images of ZCISe QDs-sensitized TiO_2 film electrode with the film thickness of 12 μm. From the high-magnification SEM images in Figure 2c, it can be seen that the TiO_2 film electrodes are composed of numerous mesoporous, which allows the fluent diffusion of electrolyte solution.[45]

Photovoltaic Performance. To suppress the charge recombination loss at the photoanode/electrolyte interfaces in assembled cell devices, a thin passivation layer of ZnS is overcoated around the surface of photoanodes, as done in a standard QDSC.[44,46] The treated photoanodes are assembled into a sandwich-type QDSC device with the use of Cu_2S/brass counter electrode and polysulfide redox electrolyte. To minimize the measurement deviation, at least five devices are prepared and tested in parallel. To obtain higher efficiency of QDSCs, we investigate systematically the influence of a series of experimental variables, including the amount of QDs used in TiO_2 suspension for the preparation of TiO_2/QD composite, and the film thickness.

Figure 3a shows the photocurrent−voltage (J−V) curves of cells under the irradiation of 1 full sun intensity based on different amounts of QDs in the preparation of TiO_2/QD composite powder. The measured short-circuit current density J_{sc} values (9.19−11.11 mA/cm^2) are consistent with the integrated current density (8.95−10.84 mA/cm^2) based on incident photon-to-current efficiency (IPCE) spectra in Figure 3b. Photovoltaic parameters (V_{oc}, J_{sc}, fill factor (FF), and PCE) that are obtained from the J−V curves are listed in Table 1. The individual photovoltaic parameters of each tested cell based on the solar paint containing different amounts of QDs are listed in Table S1. When the amount of QDs in the TiO_2 suspension is increased from 45.0 to 75.0 mg, the V_{oc}, J_{sc}, and PCE values are increased systematically, whereas the FF values are kept nearly constant. With further increase in the QD amount, the

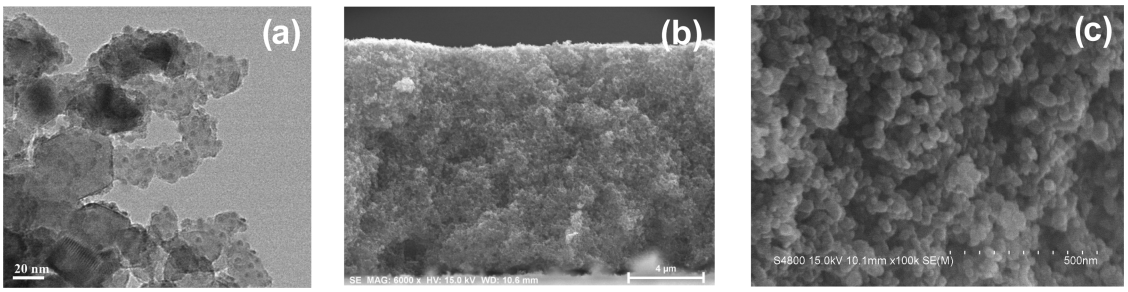

Figure 2. (a) TEM images of TiO_2 nanoparticles supported QDs. (b) Low-magnification and (c) high-magnification SEM images of the cross section of QD-sensitized TiO_2 film.

DOI: 10.1021/acsomega.7b01761
ACS Omega 2018, 3, 1102−1109

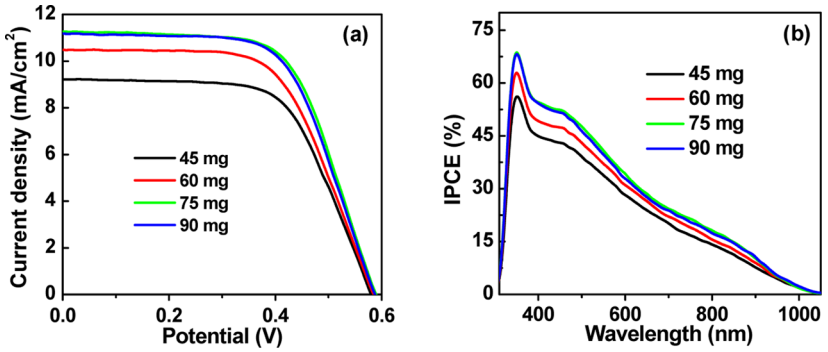

Figure 3. (a) $J-V$ and (b) IPCE curves of QDSCs corresponding to different contents of ZCISe QDs in TiO_2 suspension.

Table 1. Average Photovoltaic Performance and Standard Deviation Extracted from $J-V$ Measurement Curves of QDSCs Corresponding to Different Contents of ZCISe QDs in the TiO_2 Suspension[a]

content (mg)	V_{oc} (V)	J_{sc} (mA/cm^2)	FF	PCE (%)
45	0.576 (0.578)	9.19 (9.47)	0.632 (0.625)	3.34 ± 0.09 (3.42)
60	0.584 (0.586)	10.56 (10.88)	0.620 (0.610)	3.82 ± 0.04 (3.89)
75	0.590 (0.599)	11.11 (11.08)	0.631 (0.634)	4.13 ± 0.07 (4.21)
90	0.589 (0.590)	11.06 (11.58)	0.635 (0.626)	4.12 ± 0.11 (4.25)

[a]The numbers in parentheses represent the values obtained from the champion cells.

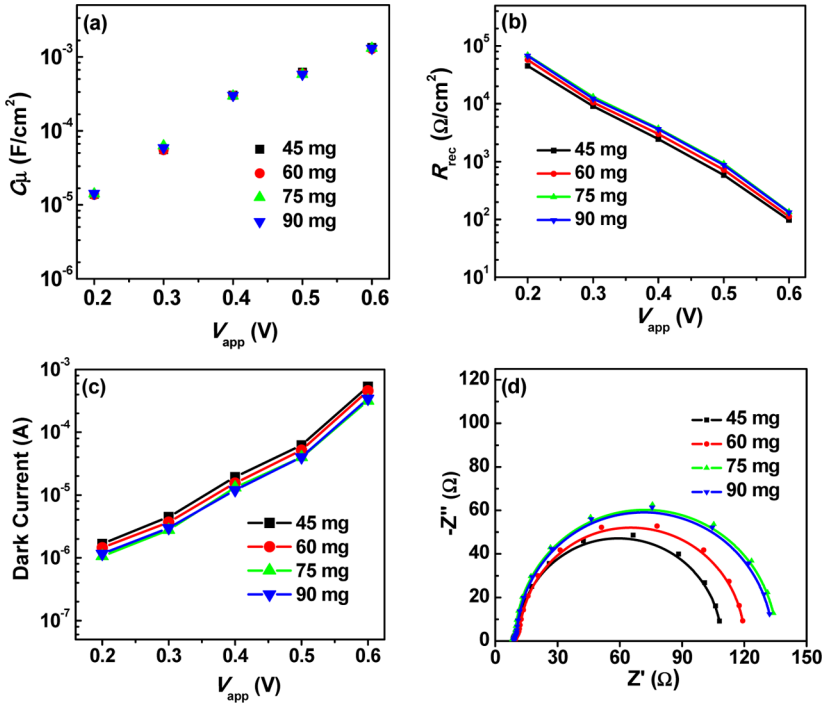

Figure 4. EIS characterization of QDSCs corresponding to different contents of ZCISe QDs in the TiO_2 suspension: (a) chemical capacitance C_μ; (b) recombination resistance R_{rec}; (c) dark current on corrected voltage V_{app}; (d) Nyquist plots at the forward bias of −0.6 V.

photovoltaic performance is kept at a plateau value. It is noted that the unabsorbed free QDs could be reused, and this accords with the concept of "green" chemistry. What is more, this method is demonstrated to be beneficial for the fabrication of larger-sized device. We have constructed the cells with a larger active area of 1.0 cm^2 and an average PCE of 3.83% was obtained, which is comparable with that of the small-sized cells. The detailed photovoltaic parameters are shown in Table S4.

The relatively low efficiency obtained in this work can be attributed to the low J_{sc} value. This work highlights a facile approach to prepare the QD-sensitized photoanode in QDSCs using a solar paint and without a need of high-temperature treatment. Nevertheless, the thickness of the photoanode film is limited in this method, which will be discussed in the following sections. What is more, the residual PVDF in the film arising from the low annealing temperature for the preparation of film electrodes also leads to the relatively low J_{sc} values.

Electrochemical Impedance Spectroscopy. To unveil the inherent mechanism for the dependence of photovoltaic performance on the amounts of QDs used in the preparation of TiO_2/QD composite, electrochemical impedance spectroscopy (EIS) is employed. All of the cell samples are measured at

DOI: 10.1021/acsomega.7b01761
ACS Omega 2018, 3, 1102−1109

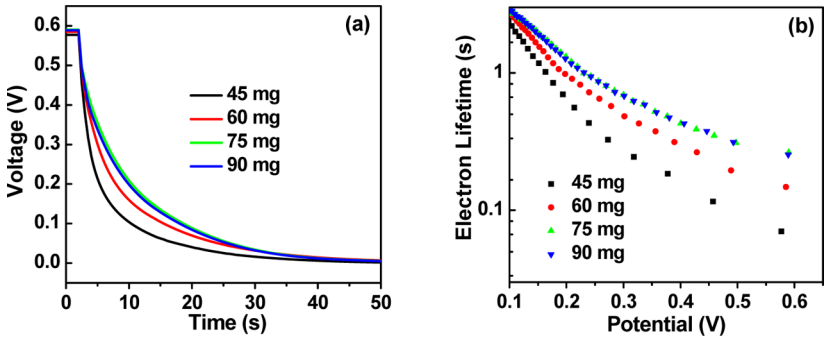

Figure 5. (a) OCVD curves of QDSCs corresponding to different contents of ZCISe QDs in the TiO_2 suspension. (b) Electron lifetime derived from OCVD measurements.

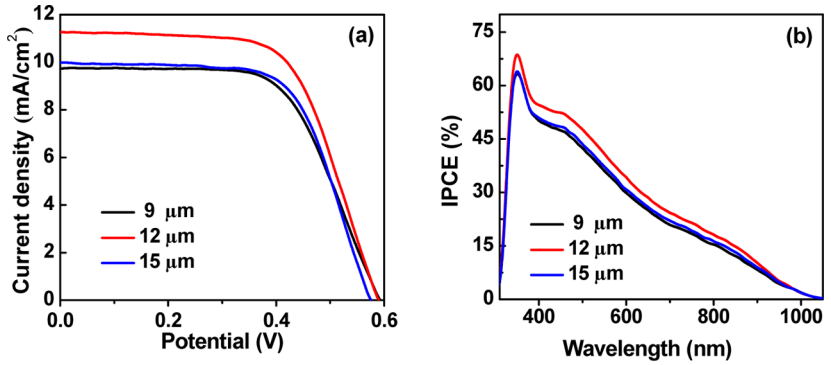

Figure 6. (a) $J-V$ and (b) IPCE curves of QDSCs based on different thicknesses of photoanode film.

different forward biases (from −0.2 to −0.6 V) under darkness. The corresponding parameters of EIS are obtained relying on the standard equivalent circuit model.[47,48] Figure 4a–c shows the applied forward bias voltage (V_{app}) dependent chemical capacitance (C_μ), recombination resistance (R_{rec}), and dark current. The similar C_μ values (Figure 4a) of all of the cells illustrate that different QD loading amounts did not change the state of the conduction band or the distribution of traps states of the TiO_2 substrate. However, with the increase in the loading amount, the R_{rec} values (Figure 4b) are improved gradually. It is well known that the charge recombination rate occurring at the photoanode/electrolyte interfaces is inversely proportional to the R_{rec} value.[49,50] With the increase in the QD loading amount, a higher surface coverage for the TiO_2 matrix is achieved, and the surface areas exposed directly to the electrolyte solution is decreased.[9] It is noted that the uncovered TiO_2 surface could act as a recombination center for the capture of photogenerated electron by the oxidized species (i.e., S_n^{2-}) in the electrolyte.[51,52] Therefore, the improvement in surface coverage favored the suppression of charge recombination process occurring at photoanode/electrolyte interfaces and brought forward the enhancement of photovoltaic performance of the resultant cell devices. Furthermore, the dependence of dark current on V_{app} as shown in Figure 4c gives further support for the suppressed charge recombination rate with the increase in the QD loading amount. To distinguish the recombination difference of cells based on different QD loading amounts, Figure 4d shows the Nyquist plots of the corresponding cells under the forward bias near the V_{oc} value. The observed greater diameter for the semicircles corresponding to larger QD loading amount indicates a greater charge recombination resistance. Overall, the EIS results indicate that the charge recombination occurring at TiO_2/QDs/electrolyte interfaces is inhibited with an increase in the loading amount of QD on the TiO_2 particles. The EIS results are in well-accordance with the results from the $J-V$ measurements as shown in Table 1 and Figure 3.

Open-Circuit Voltage Decay. To illustrate further the performance difference of the cells based on different amounts of QDs in film electrodes, the open-circuit voltage decay (OCVD) measurement is used to analyze the electron recombination processes. A white light-emitting diode of 100 mW/cm^2 continuously illuminates on the studied cell to get to a stable voltage, and then the open-circuit voltage decay information is recorded after switching off the light.[53,54] As shown in Figure 5a, it can be seen that the rate of voltage decay becomes slower by increasing the amount of QDs. The electron lifetime (τ_n) can be visually reflected by the open-circuit voltage decay curves. Figure 5b shows the electron lifetime, which can be calculated using the equation $\tau_n = -(k_B T/e)(dV_{oc}/dt)^{-1}$, where k_B, T, and e are the Boltzmann constant, the absolute temperature (298 K), and the electronic charge, respectively.[45] From Figure 5, it is obvious that the solar cells based on a higher QD loading amount correspond to a longer electron lifetime related to those with a lesser QD loading amount at the identical potential, indicating that the charge recombination process is retarded by the increasing QD loading amount. This observation is consistent with that observed in the EIS measurement, and therefore gives further evidence for the obtained better photovoltaic performance as observed from the $J-V$ measurements.

Effect of Film Thickness on Photovoltaic Performance. In addition to the different amounts of QDs in the solar paint, the mesoporous film thickness of a photoanode is another important parameter in determining the performance of the resulting cell devices. In a certain range, a thicker film can

DOI: 10.1021/acsomega.7b01761
ACS Omega 2018, 3, 1102−1109

Table 2. Average Photovoltaic Parameters of QDSCs Based on Different Thicknesses of Photoanode Film[a]

thickness (μm)	V_{oc} (V)	J_{sc} (mA/cm^2)	FF	PCE (%)
9	0.598 (0.601)	9.99 (10.22)	0.615 (0.614)	3.67 ± 0.08 (3.77)
12	0.590 (0.599)	11.11 (11.08)	0.631 (0.634)	4.13 ± 0.07 (4.21)
15	0.585 (0.589)	10.01 (10.13)	0.639 (0.640)	3.74 ± 0.06 (3.82)

[a]The numbers in parentheses represent the values obtained from the champion cells.

enhance the light absorption capacity and thus improve the photocurrent, whereas it will increase the possibility of a charge recombination simultaneously.[55] In the experiment for optimizing film thickness, the amounts of QDs and PVDF in the solar paint is kept at an optimum value. The $J-V$ and IPCE curves for champion cells under variable film thickness are shown in Figure 6. As shown in Table 2, the average photovoltaic performances (V_{oc}, J_{sc}, FF, and PCE) are improved with the increase in the film thickness from 9 to 12 μm. The individual photovoltaic parameters of each tested cell with different film thickness are displayed in Table S2. We can see that the improved PCE is mainly derived from the increased J_{sc}. When the film thickness is increased furthermore from 12 to 15 μm, V_{oc}, J_{sc}, and PCE are decreased; however, the FF is increased. This demonstrates that the photovoltaic performance of the resulting cell device could not be improved by just monotonously increasing the thickness of the photoanode film. Furthermore, our experiment results indicate that the strength of the photoanode film is sacrificed with an increase in the thickness of the film, and the resulting thick film is easier to fall off from the FTO glass substrate. Our experimental results indicate that the thickness of 12 μm is the optimized value in consideration of both photovoltaic performance and device stability.

CONCLUSIONS

In summary, a transformative approach for the preparation of QD-sensitized photoanode in QDSCs was developed by simply brushing a solar paint on the FTO conductive glass. The solar paint was derived from the TiO_2/QD composite, which can be obtained in a time period as short as half minute by mixing the initial oil-soluble QDs and TiO_2 P25 suspension. Obviously, this approach can simplify the preparation process of QD-sensitized photoanodes, especially the QD sensitization step, and, therefore, speed up the industrialization process of QDSCs. An average PCE of 4.13% (V_{oc} = 0.590 V, J_{sc} = 11.11 mA/cm^2, FF = 0.631) was achieved on ZCISe QDSCs prepared through this solar paint approach. Further optimization of the solar paint composition and other components of the device are necessary to boost further the performance of the resultant cell devices.

EXPERIMENTAL SECTION

Chemicals. Selenium powder (200 mesh, 99.99%), oleylamine (OAm, 95%), 1-octadecene (90%), and poly(vinylidene difluoride) (PVDF) were purchased from Aldrich. Diphenylphosphine (98%) and zinc acetate ($Zn(OAc)_2$, 99.99%) were obtained from J&K. Copper iodide (CuI, 99.998%) and indium acetate ($In(OAc)_3$) were received from Alfa Aesar. P25 powder (20% rutile and 80% anatase) was obtained from Degussa. All of the chemicals were used as received without further treatment.

Preparation of Solar Paint and Fabrication of Solar Cells. The procedure and all of the chemicals used for the preparation of oil-soluble ZCISe QDs were identical to previous report.[32] The TiO_2/QD composites were obtained by simply mixing the as-prepared oil-soluble QDs with TiO_2 P25 nanoparticles suspension in the dichloromethane medium. Typically, 10.0 mL of P25 suspension in dichloromethane (containing 0.5 g of P25) was mixed with an equal volume of as-prepared ZCISe QD dispersion in dichloromethane (containing 75.0 mg of ZCISe QDs), and the resulting mixture was subjected to sonication for 30 s to complete the process of adsorption of QDs on the surface of TiO_2 particles. The TiO_2/QDs powder was collected via a centrifugation/precipitation process for twice to get rid of the unattached free-dispersion QDs in solution. The powder product was then dried under hot air with typical yields of 0.571 g.

Binder solution for the following solar paint was prepared according to standard literature method.[36] In the procedure for solar paint preparation, the obtained TiO_2/QD powder (0.571 g), 1.0 mL as-prepared binder solution were loaded to a mixture containing 6.0 mL of anhydrous ethanol and 100 μL of TiO_2-sol in a 50 mL round-bottom flask and then sonicated for 10 min. The solar paint was obtained by the removal of redundant ethanol from this mixture through a rotary evaporation process.

The photoanode film were fabricated by screen-printing the obtained solar paint on a FTO glass (8 Ω/sq) and then sintered at 120 °C for 60 min in a muffle-type furnace at ambient atmosphere. The sandwich-type cells were fabricated by assembling the Cu_2S/brass counter electrode and the photoanode film using a scotch spacer (50 μm). Modified polysulfide aqueous solution containing 2.0 M of S, 2.0 M Na_2S, and 20 wt % poly(vinyl pyrrolidone) was used as redox electrolyte.[37]

Characterization. The morphology of the photoanode film was studied by a Hitachi S4800 SEM. The TEM images were obtained on a JEOL JEM-2100 instrument with an operation voltage of 200 kV. The absorption spectra of the photoanode film were measured on a Shimadzu UV-2600 spectrometer. The Keithley 2000 multimeter with illumination from a 300 W tungsten lamp with a Spectral Product DK240 monochromator was used to measure IPCE curves. The $J-V$ characteristics of the cell devices were recorded on a Keithley 2400 source meter under illumination of simulated AM 1.5G solar light (Oriel, model no. 94022A). A NREL standard silicon solar cell was used to calibrate the light intensity before each measurement. The photoactive area was determined by a black metal mask of 0.237 cm^2. OCVD and EIS were obtained using an electrochemical workstation (Zahner, Zennium).

ASSOCIATED CONTENT

Supporting Information

The Supporting Information is available free of charge on the ACS Publications website at DOI: 10.1021/acsomega.7b01761.

Absorption spectra of oil-soluble ZCISe QD dispersions in dichloromethane; the individual photovoltaic parameters extracted from $J-V$ measurement curves of QDSCs corresponding to different contents of ZCISe QDs in the

DOI: 10.1021/acsomega.7b01761
ACS Omega 2018, 3, 1102−1109

TiO_2 suspension; the individual photovoltaic parameters based on different thicknesses of photoanode film (PDF)

AUTHOR INFORMATION

Corresponding Authors

*E-mail: zxpan@scau.edu.cn. Tel/Fax: (+86) 20 8528 0319 (Z.P.).

*E-mail: zhongxh@ecust.edu.cn (X.Z.).

ORCID

Xinhua Zhong: 0000-0002-2062-8773

Notes

The authors declare no competing financial interest.

ACKNOWLEDGMENTS

We acknowledge the National Natural Science Foundation of China (Nos. 51732004, 91433106, and 21703071), the Fundamental Research Funds for the Central Universities in China for financial supports.

REFERENCES

(1) Green, M. A.; Bremner, S. P. Energy Conversion Approaches and Materials for High-Efficiency Photovoltaics. *Nat. Mater.* **2016**, *16*, 23−34.

(2) Carey, G. H.; Abdelhady, A. L.; Ning, Z.; Thon, S. M.; Bakr, O. M.; Sargent, E. H. Colloidal Quantum Dot Solar Cells. *Chem. Rev.* **2015**, *115*, 12732−12763.

(3) Kamat, P. V. Boosting the Efficiency of Quantum Dot Sensitized Solar Cells through Modulation of Interfacial Charge Transfer. *Acc. Chem. Res.* **2012**, *45*, 1906−1915.

(4) Albero, J.; Clifford, J. N.; Palomares, E. Quantum Dot Based Molecular Solar Cells. *Coord. Chem. Rev.* **2014**, *263*−*264*, 53−64.

(5) Yang, J.; Choi, M. K.; Kim, D.-H.; Hyeon, T. Designed Assembly and Integration of Colloidal Nanocrystals for Device Applications. *Adv. Mater.* **2016**, *28*, 1176−1207.

(6) Kamat, P. V. Quantum Dot Solar Cells. The Next Big Thing in Photovoltaics. *J. Phys. Chem. Lett.* **2013**, *4*, 908−918.

(7) Semonin, O. E.; Luther, J. M.; Choi, S.; Chen, H.-Y.; Gao, J.; Nozik, A. J.; Beard, M. C. Peak External Photocurrent Quantum Efficiency Exceeding 100% via MEG in a Quantum Dot Solar Cell. *Science* **2011**, *334*, 1530−1533.

(8) Nozik, A. J.; Beard, M. C.; Luther, J. M.; Law, M.; Ellingson, R. J.; Johnson, J. C. Semiconductor Quantum Dots and Quantum Dot Arrays and Applications of Multiple Exciton Generation to Third Generation Photovoltaic Solar Cells. *Chem. Rev.* **2010**, *110*, 6873−6890.

(9) Li, W.; Zhong, X. Capping Ligand-Induced Self-Assembly for Quantum Dot Sensitized Solar Cells. *J. Phys. Chem. Lett.* **2015**, *6*, 796−806.

(10) Du, Z.; Zhang, H.; Bao, H.; Zhong, X. Optimization of TiO_2 Photoanode Films for Highly Efficient Quantum Dot-Sensitized Solar Cells. *J. Mater. Chem. A* **2014**, *2*, 13033−13040.

(11) Ito, S.; Murakami, T. N.; Comte, P.; Liska, P.; Grätzel, C.; Nazeeruddin, M. K.; Grätzel, M. Fabrication of Thin Film Dye Sensitized Solar Cells with Solar to Electric Power Conversion Efficiency over 10%. *Thin Solid Films* **2008**, *516*, 4613−4619.

(12) Mora-Seró, I.; Bisquert, J. Breakthroughs in the Development of Semiconductor Sensitized Solar Cells. *J. Phys. Chem. Lett.* **2010**, *1*, 3046−3052.

(13) Watson, D. F. Linker-Assisted Assembly and Interfacial Electron-Transfer Reactivity of Quantum Dot−Substrate Architectures. *J. Phys. Chem. Lett.* **2010**, *1*, 2299−2309.

(14) Ye, M.; Gao, X.; Hong, X.; Liu, Q.; He, C.; Liu, X.; Lin, C. Recent Advances in Quantum Dot-sensitized Solar Cells: Insights into Photoanodes, Sensitizers, Electrolytes and Counter Electrodes. *Sustainable Energy Fuels* **2017**, *1*, 1217−1231.

(15) Lai, C.-H.; Chou, P.-T. All Chemically Deposited, Annealing and Mesoporous Metal Oxide Free CdSe Solar Cells. *Chem. Commun.* **2011**, *47*, 3448−3450.

(16) Lee, Y.-L.; Lo, Y.-S. Highly Efficient Quantum-Dot-Sensitized Solar Cell Based on Co-Sensitization of CdS/CdSe. *Adv. Funct. Mater.* **2009**, *19*, 604−609.

(17) Yu, X.-Y.; Lei, B.-X.; Kuang, D.-B.; Su, C.-Y. Highly Efficient CdTe/CdS Quantum Dot Sensitized Solar Cells Fabricated by a One Step Linker Assisted Chemical Bath Deposition. *Chem. Sci.* **2011**, *2*, 1396−1400.

(18) Lee, H.; Wang, M.; Chen, P.; Gamelin, D. R.; Zakeeruddin, S. M.; Grätzel, M.; Nazeeruddin, M. K. Efficient CdSe Quantum Dot-Sensitized Solar Cells Prepared by an Improved Successive Ionic Layer Adsorption and Reaction Process. *Nano Lett.* **2009**, *9*, 4221−4227.

(19) Lee, H. J.; Bang, J.; Park, J.; Kim, S.; Park, S.-M. Multilayered Semiconductor (CdS/CdSe/ZnS)-Sensitized TiO_2 Mesoporous Solar Cells: All Prepared by Successive Ionic Layer Adsorption and Reaction Processes. *Chem. Mater.* **2010**, *22*, 5636−5643.

(20) Santra, P. K.; Kamat, P. V. Mn-Doped Quantum Dot Sensitized Solar Cells: A Strategy to Boost Efficiency over 5%. *J. Am. Chem. Soc.* **2012**, *134*, 2508−2511.

(21) Zaban, A.; Mićić, O. I.; Gregg, B. A.; Nozik, A. J. Photosensitization of Nanoporous TiO_2 Electrodes with InP Quantum Dots. *Langmuir* **1998**, *14*, 3153−3156.

(22) Smith, N. J.; Emmett, K. J.; Rosenthal, S. J. Photovoltaic Cells Fabricated by Electrophoretic Deposition of CdSe Nanocrystals. *Appl. Phys. Lett.* **2008**, *93*, No. 043504.

(23) Brown, P.; Kamat, P. V. Quantum Dot Solar Cells. Electrophoretic Deposition of CdSe-C_{60} Composite Films and Capture of Photogenerated Electrons with nC_{60} Cluster Shell. *J. Am. Chem. Soc.* **2008**, *130*, 8890−8891.

(24) Salant, A.; Shalom, M.; Hod, I.; Faust, A.; Zaban, A.; Banin, U. Quantum Dot Sensitized Solar Cells with Improved Efficiency Prepared Using Electrophoretic Deposition. *ACS Nano* **2010**, *4*, 5962−5968.

(25) Yu, X.-Y.; Liao, J.-Y.; Qiu, K.-Q.; Kuang, D.-B.; Su, C.-Y. Dynamic Study of Highly Efficient CdS/CdSe Quantum DotSensitized Solar Cells Fabricated by Electrodeposition. *ACS Nano* **2011**, *5*, 9494−9500.

(26) Zhang, H.; Cheng, K.; Hou, Y.; Fang, Z.; Pan, Z.; Wu, W.; Hua, J.; Zhong, X. Efficient CdSe Quantum Dot-Sensitized Solar Cells Prepared by a Postsynthesis Assembly Approach. *Chem. Commun.* **2012**, *48*, 11235−11237.

(27) Wang, W.; Jiang, G.; Yu, J.; Wang, W.; Pan, Z.; Nakazawa, N.; Shen, Q.; Zhong, X. High Efficiency Quantum Dot Sensitized Solar Cells Based on Direct Adsorption of Quantum Dots on Photoanodes. *ACS Appl. Mater. Interfaces* **2017**, *9*, 22549−22559.

(28) Hod, I.; Zaban, A. Materials and Interfaces in Quantum Dot Sensitized Solar Cells: Challenges, Advances and Prospects. *Langmuir* **2014**, *30*, 7264−7273.

(29) Pan, Z.; Zhao, K.; Wang, J.; Zhang, H.; Feng, Y.; Zhong, X. Near Infrared Absorption of $CdSe_xTe_{1-x}$ Alloyed Quantum Dot Sensitized Solar Cells with More than 6% Efficiency and High Stability. *ACS Nano* **2013**, *7*, 5215−5222.

(30) Zhao, K.; Pan, Z.; Mora-Seró, I.; Cánovas, E.; Wang, H.; Song, Y.; Gong, X.; Wang, J.; Bonn, M.; Bisquert, J.; Zhong, X. Boosting Power Conversion Efficiencies of Quantum-Dot-Sensitized Solar Cells Beyond 8% by Recombination Control. *J. Am. Chem. Soc.* **2015**, *137*, 5602−5609.

(31) Wang, G.; Wei, H.; Shi, J.; Xu, Y.; Wu, H.; Luo, Y.; Li, D.; Meng, Q. Significantly Enhanced Energy Conversion Efficiency of $CuInS_2$ Quantum Dot Sensitized Solar Cells by Controlling Surface Defects. *Nano Energy* **2017**, *35*, 17−25.

(32) Du, J.; Du, Z.; Hu, J.-S.; Pan, Z.; Shen, Q.; Sun, J.; Long, D.; Dong, H.; Sun, L.; Zhong, X.; Wan, L.-J. Zn-Cu-In-Se Quantum Dot Solar Cells with a Certified Power Conversion Efficiency of 11.6%. *J. Am. Chem. Soc.* **2016**, *138*, 4201−4209.

DOI: 10.1021/acsomega.7b01761
ACS Omega 2018, 3, 1102−1109

(33) Hodes, G.; Cahen, D.; Manassen, J.; David, M. Painted, Polycrystalline Thin Film Photoelectrodes for Photoelectrochemical Solar Cells. *J. Electrochem. Soc.* **1980**, *127*, 2252−2254.
(34) Genovese, M. P.; Lightcap, I. V.; Kamat, P. V. Sun-Believable Solar Paint. A Transformative One-Step Approach for Designing Nanocrystalline Solar Cells. *ACS Nano* **2012**, *6*, 865−872.
(35) Abbas, M. A.; Basit, M. A.; Yoon, S. J.; Lee, G. J.; Lee, M. D.; Park, T. J.; Kamat, P. V.; Bang, J. H. Revival of Solar Paint Concept: Air-Processable Solar Paints for the Fabrication of Quantum Dot-Sensitized Solar Cells. *J. Phys. Chem. C* **2017**, *121*, 17658−17670.
(36) Du, Z.; Tong, J.; Guo, W.; Zhang, H.; Zhong, X. Cuprous Sulfide on Ni Foam as a Counter Electrode for Flexible Quantum Dot Sensitized Solar Cells. *J. Mater. Chem. A* **2016**, *4*, 11754−11761.
(37) Jiang, G.; Pan, Z.; Ren, Z.; Du, J.; Yang, C.; Wang, W.; Zhong, X. Poly(vinyl pyrrolidone): A Superior and General Additive in Polysulfide Electrolytes for High Efficiency Quantum Dot Sensitized Solar Cells. *J. Mater. Chem. A* **2016**, *4*, 11416−11421.
(38) Panthani, M. G.; Stolle, C. J.; Reid, D. K.; Rhee, D. J.; Harvey, T. B.; Akhavan, V. A.; Yu, Y.; Korgel, B. A. $CuInSe_2$ Quantum Dot Solar Cells with High Open-Circuit Voltage. *J. Phys. Chem. Lett.* **2013**, *4*, 2030−2034.
(39) Guijarro, N.; Lana-Villarreal, T.; Mora-Seró, I.; Bisquert, J.; Gómez, R. CdSe Quantum Dot-Sensitized TiO_2 Electrodes: Effect of Quantum Dot Coverage and Mode of Attachment. *J. Phys. Chem. C* **2009**, *113*, 4208−4214.
(40) Giménez, S.; Mora-Seró, I.; Macor, L.; Guijarro, N.; Lana-Villarreal, T.; Gómez, R.; Diguna, L. J.; Shen, Q.; Toyoda, T.; Bisquert, J. Improving the Performance of Colloidal Quantum-dot-sensitized Solar Cells. *Nanotechnology* **2009**, *20*, No. 295204.
(41) Fuke, N.; Hoch, L. B.; Koposov, A. Y.; Manner, V. W.; Werder, D. J.; Fukui, A.; Koide, N.; Katayama, H.; Sykora, M. CdSe Quantum Dot-Sensitized Solar Cell with ∼100% Internal Quantum Efficiency. *ACS Nano* **2010**, *4*, 6377−6386.
(42) McDaniel, H.; Fuke, N.; Makarov, N. S.; Pietryga, J. M.; Klimov, V. I. An Integrated Approach to Realizing High-Performance Liquid Junction Quantum Dot Sensitized Solar Cells. *Nat. Commun.* **2013**, *4*, No. 2887.
(43) Guijarro, N.; Guillén, E.; Lana-Villarreal, T.; Gómez, R. Quantum Dot-Sensitized Solar Cells Based on Directly Adsorbed Zinc Copper Indium Sulfide Colloids. *Phys. Chem. Chem. Phys.* **2014**, *16*, 9115−9122.
(44) Kim, J.-Y.; Yang, J.; Yu, J. H.; Baek, W.; Lee, C.-H.; Son, H. J.; Hyeon, T.; Ko, M. J. Highly Efficient Copper-Indium-Selenide Quantum Dot Solar Cells: Suppression of Carrier Recombination by Controlled ZnS Overlayers. *ACS Nano* **2015**, *9*, 11286−11295.
(45) Bisquert, J.; Zaban, A.; Greenshtein, M.; Mora-Seró, I. Determination of Rate Constants for Charge Transfer and the Distribution of Semiconductor and Electrolyte Electronic Energy Levels in Dye-Sensitized Solar Cells by Open-Circuit Photovoltage Decay Method. *J. Am. Chem. Soc.* **2004**, *126*, 13550−13559.
(46) Pan, Z.; Mora-Seró, I.; Shen, Q.; Zhang, H.; Li, Y.; Zhao, K.; Wang, J.; Zhong, X.; Bisquert, J. High-Efficiency "Green" Quantum Dot Solar Cells. *J. Am. Chem. Soc.* **2014**, *136*, 9203−9210.
(47) Pan, Z.; Zhong, X. A ZnS and Metal Hydroxide Composite Passivation Layer for Recombination Control in High Efficiency Quantum Dot Sensitized Solar Cells. *J. Mater. Chem. A* **2016**, *4*, 18976−18982.
(48) Zhang, L.; Pan, Z.; Wang, W.; Du, J.; Ren, Z.; Shen, Q.; Zhong, X. Copper Deficient Zn−Cu−In−Se Quantum Dot Sensitized Solar Cells for High Efficiency. *J. Mater. Chem. A* **2017**, *5*, 21442−21451.
(49) Samadpour, M.; Boix, P. P.; Giménez, S.; Zad, A. I.; Taghavinia, N.; Mora-Seró, I.; Bisquert, J. Fluorine Treatment of TiO_2 for Enhancing Quantum Dot Sensitized Solar Cell Performance. *J. Phys. Chem. C* **2011**, *115*, 14400−14407.
(50) González-Pedro, V.; Xu, X.; Mora- Seró, I.; Bisquert, J. Modeling High-Efficiency Quantum Dot Sensitized Solar Cells. *ACS Nano* **2010**, *4*, 5783−5790.
(51) Tachan, Z.; Hod, I.; Shalom, M.; Grinis, L.; Zaban, A. The Importance of the TiO_2/Quantum Dots Interface in the Recombination Processes of Quantum Dot Sensitized Solar Cells. *Phys. Chem. Chem. Phys.* **2013**, *15*, 3841−3845.
(52) Zhao, K.; Pan, Z.; Zhong, X. Charge Recombination Control for High Efficiency Quantum Dot Sensitized Solar Cells. *J. Phys. Chem. Lett.* **2016**, *7*, 406−417.
(53) Wu, W.-Q.; Liao, J.-Y.; Chen, H.-Y.; Yu, X.-Y.; Su, C.-Y.; Kuang, D.-B. Dye-Sensitized Solar Cells Based on a Double Layered TiO_2 Photoanode Consisting of Hierarchical Nanowire Arrays and Nanoparticles with Greatly Improved Photovoltaic Performance. *J. Mater. Chem.* **2012**, *22*, 18057−18062.
(54) Zhang, M.; Zhang, J.; Fan, Y.; Yang, L.; Wang, Y.; Li, R.; Wang, P. Judicious Selection of a Pinhole Defect Filler to Generally Enhance the Performance of Organic Dye-Sensitized Solar Cells. *Energy Environ. Sci.* **2013**, *6*, 2939−2943.
(55) Vogel, R.; Hoyer, P.; Weller, H. Quantum-Sized PbS, CdS, Ag_2S, Sb_2S_3, and Bi_2S_3 Particles as Sensitizers for Various Nanoporous Wide Bandgap Semiconductors. *J. Phys. Chem.* **1994**, *98*, 3183−3188.

DOI: 10.1021/acsomega.7b01761
ACS Omega 2018, 3, 1102−1109